Fluoride ion sensing with an acridinium borane;

Wei-Chun Liu and François P. Gabbaï*

Department of Chemistry, Texas A&M University, College Station, Texas 77843, USA

Abstract

With our continuing interest in the chemistry of cationic boranes, we have synthesized the

tetrafluoroborate salt of 1-dimesitylboron-4-(N-methyl-9-acridinium)-phenylene which acts as a

turn-on fluoride anion sensor, visibly changing from yellow to orange upon binding fluoride. To

understand this reactivity, we spectroscopically and computationally analyzed the cation and

triarylfluoroborate adduct. UV-vis spectroscopy and TD-DFT revealed the basis of the color

change to be a red shift in a low-energy absorption band resulting from intramolecular charge-

Electrochemical studies were undertaken to further probe this system. Cyclic transfer.

voltammetry indicated a reversible one-electron reduction for the cation and a cathodic shift of -

0.12 V in the first reduction wave upon fluoride binding. Chemical reduction of the cation

yielded the acridine borane radical which was verified by EPR spectroscopy.

Keywords: Boron, carbenium, fluoride ion sensing, acridine radical

*Corresponding author. Email: francois@tamu.edu

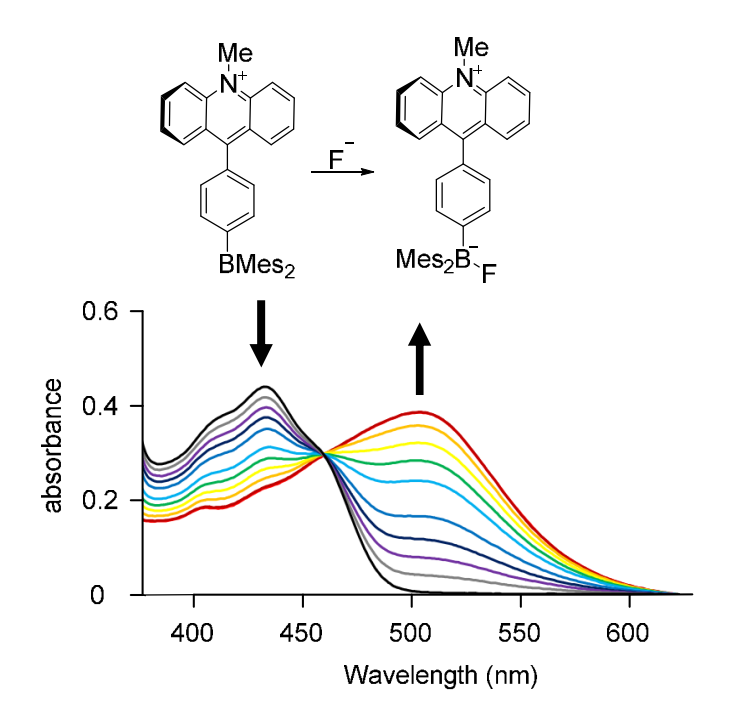
† This paper is dedicated to the memory of Suning Wang, whose contributions have inspired

much of our efforts in boron and late transition metal chemistry.

‡ The Supporting Information contains additional experimental, characterization and

computational details. Crystallographic details in CIF format are also available.

Graphical Abstract



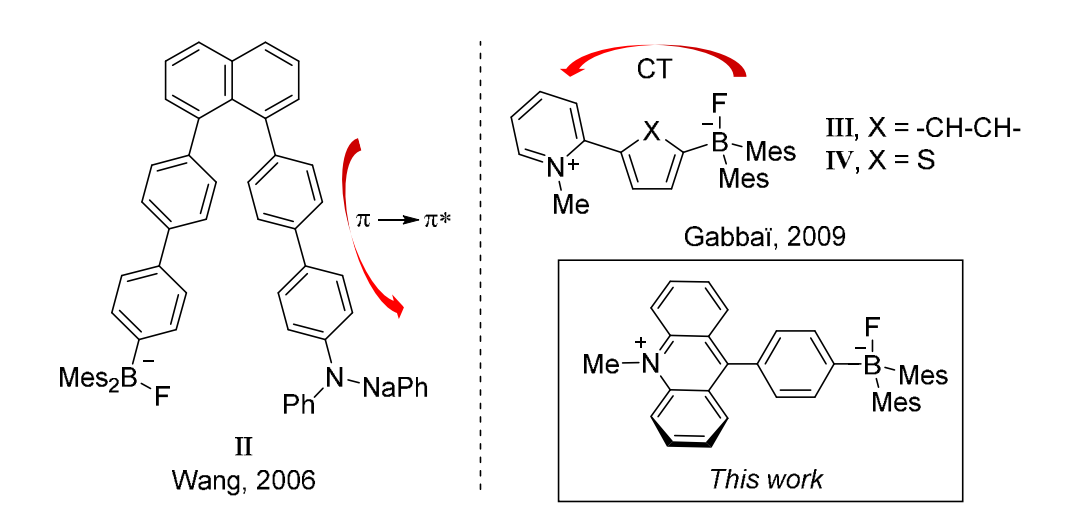
1. Introduction

Fluoride anion recognition has become an attractive research area in recent decades due to concerns regarding this anion's potential toxicity to humans and the environment.¹⁻³ One conventional approach in detecting this anion is to use a chemosensor containing a Lewis acid such as a triarylborane (Scheme 1. Left: Application of triarylboranes in fluoride anion sensing. Right: Example of a cationic borane in fluoride binding.left). In aprotic organic solvents, these boranes demonstrate high fluorophilicity with anion binding constants in the range of 10⁵ to 10⁶ M⁻¹; however, low fluoride binding constants in protic media limits these complexes' practical application.⁴⁻⁶ In attempts to augment the binding affinity through favorable coulombic attractions, a series of boranes containing positively charged moieties such as pyridinium,⁷ phosphonium,⁸⁻¹⁰ or cationic transition metals^{11, 12} were explored. For example, the phosphonium borane [I]⁺ binds fluoride in aqueous solutions where the anion is highly hydrated (Scheme 1, right).

$$Ar \xrightarrow{B} Ar \xrightarrow{F} Ar \xrightarrow{Ar} Ar \xrightarrow{B} Ar = \begin{bmatrix} II]^+ \end{bmatrix}$$
 $Ar \xrightarrow{B} Ar \xrightarrow{B} Ar \xrightarrow{Ar} Ar = \begin{bmatrix} II]^+ \end{bmatrix}$
 $F \xrightarrow{PPh_3} F \xrightarrow$

Scheme 1. Left: Application of triarylboranes in fluoride anion sensing. Right: Example of a cationic borane in fluoride binding.

In most cases, fluoride complexation by triarylboranes is accompanied by a quenching of the boron-centered chromophore, leading to a turn-off response to fluoride sensing. However, turnon sensing would be more practical in application due to its higher sensitivity.^{4, 13, 14} Following this idea, Wang and co-workers described a family of bifunctional moleucles including II containing triarylamine and triarylborane moieties (Scheme 2).^{13, 15} Addition of fluoride to the boron center of II revived an intense $\pi \to \pi^*$ charge transfer (CT) band in the triarylamine moiety, producing a turn-on colorimetric response. A similar turn-on behavior was also found in the case of pyridinium boranes such as III and IV (Scheme 2).⁷ A through-space charge-transfer from the borane to the pyridinium moiety was detected upon conversion of the borane into a fluoroborate, shifting the electronic transition to the visible region.



Scheme 2. Examples of turn-on intramolecular CT after fluoride ion binding

Inspired by these examples, our group decided to further the study of such bifunctional systems in anion sensing. In this work, we describe a dimesityl phenyl borane posessing an acridinium chromophore, [2]BF₄. We studied this complex's reactivity toward fluoride using UV-vis spectroscopy, and we investigated the redox properties of [2]BF₄ and its fluoride-adduct, 2-F, to explore an electrochemical response of fluoride binding.

2. Synthesis of compound 1 and [2]BF₄

To begin, we synthesized carbinol **1** by lithiating (4-bromophenyl)dimesitylborane and quenching the salt with *N*-methylacridone. The desired carbinol was afforded as a white solid in 73% yield after aqueous work up (Scheme 3). Carbinol **1** was fully characterized by NMR spectroscopy and structurally confirmed using X-ray diffraction (XRD) analysis (Figure 1 and Table 1). Subsequent reaction with aqueous HBF₄ yielded [**2**]BF₄ as an air-stable, yellow salt. The ¹H NMR spectrum revealed a significant downfield shift of the acridine resonances when compared to those of carbinol **1**. With a broad resonance at 75.8 ppm, the ¹¹B NMR spectrum of [**2**]BF₄ is diagnostic of a free triaryl borane. ¹⁶

Scheme 3. Synthesis of 1 and [2]BF₄.

The crystal structure of [2]BF₄ was also determined. The boron B(1) and carbenium carbon C(9) centers adopt a trigonal planar geometry ($\Sigma_{\angle C-B-C} = 360.0^{\circ}$, $\Sigma_{\angle C-C-C} = 359.9^{\circ}$) and do not form short contacts with the counteranions. As expected, the dimesitylboryl moiety is efficiently π -conjugated with the p-phenylene backbone as evidenced by the relatively small dihedral angle of 23.7° between the planes containing C(21)-B(1)-C(30) and C(17)-C(18)-C(19), respectively. On

the other hand, the dihedral angle of 65.4° formed by the C(10)-C(9)-C(12) and C(16)-C(15)-C(20) planes indicates reduced conjugation of the acridinium unit with the rest of the molecule.

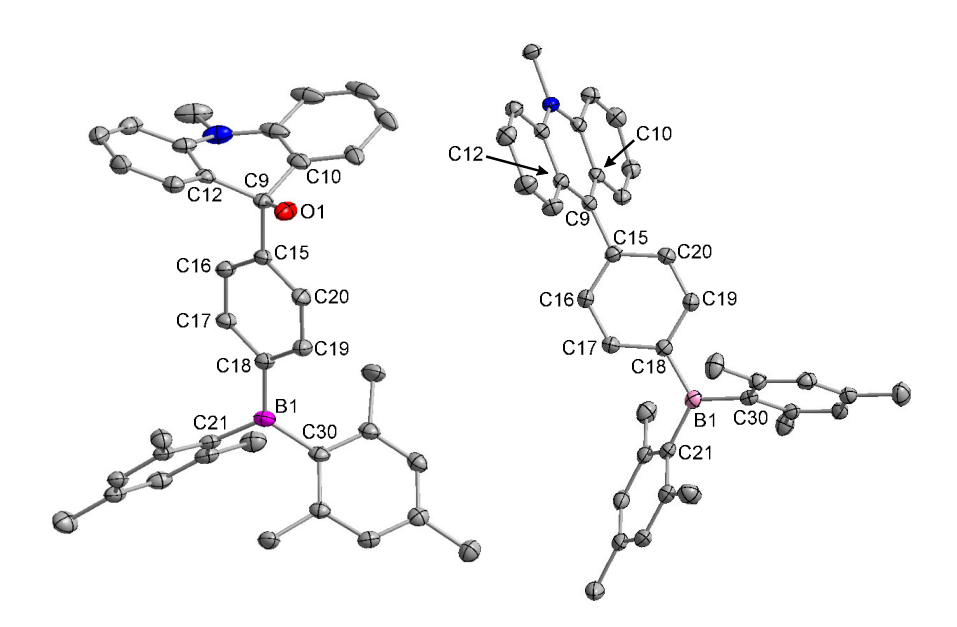


Figure 1. Solid-state structures of 1 (left) and [2]BF₄ (right). Hydrogen atoms and counter anions are omitted for clarity. Thermal ellipsoids are set at 50% probability.

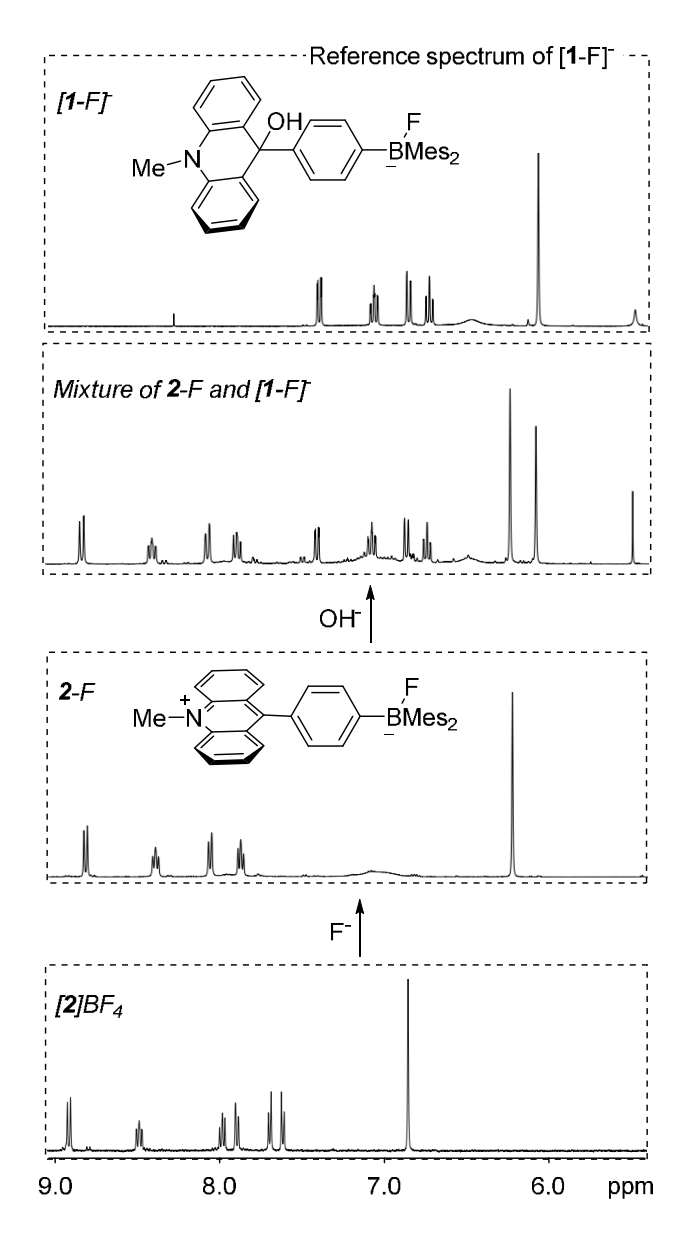
Table 1. Crystal Data, Data Collection, and Structure Refinement for 1 and [2]BF₄.

Crystal data	1	[2]BF ₄
Formula	C ₃₈ H ₃₈ BNO	$C_{37}H_{37}B_2F_4N$
$M_{ m r}$	535.50	605.30
crystal size (mm ³)	0.23 x 0.16 x 0.09	0.18 x 0.16 x 0.11
crystal system	Monoclinic	Monoclinic
space group	P2(1)/c	P2(1)/c
a (Å)	8.4527(4)	14.6542(4)
b (Å)	12.5757(6)	18.8072(5)
c (Å)	27.8354(13)	11.6308(3)
α (°)	90	90
β (°)	91.374(2)	103.4500(10)
γ (°)	90	90
$V(Å^3)$	2958.0(2)	3117.58(14)
Z	4	4
$ ho_{ m calc}$ (g cm ⁻³)	1.202	1.290
$\mu (\mathrm{mm}^{-1})$	0.070	0.730
F(000)	1144	1272
Data Collection		

T(K)	110.0	110.0
Scan mode	W	W
	-11 → +11,	-16 → +17,
hkl range	-17 → +17 ,	-22 → +22,
	-38 → +38	-14 → +14
measd reflns	88126	88607
unique reflns $[R_{int}]$	8303 [0.1182]	5703 [0.0364]
reflns used for refinement	8303	5703
Refinement		
refined parameters	381	413
GooF	1.049	1.045
R1, wR2 all data	0.1165, 0.1679	0.0396, 0.0943
$ ho_{ m fin}$ (max/min) (e Å-3)	0.30, -0.30	0.23, -0.18

3. Fluoride anion binding by [2]BF₄

With these boranes in hand, we next investigated their reactivity with fluoride. Upon adding tetrabutylammonium fluoride trihydrate (TBAF•3H₂O) to a CH₂Cl₂ solution of [2]BF₄, the fluoroborate adduct 2-F was obtained as an orange powder (Scheme 4). This orange solid was insoluble in organic solvents such as CH₂Cl₂, CHCl₃, MeCN, and MeOH and was only slightly soluble in DMSO. NMR analysis verified the presence of the triarylfluoroborate unit with distinct chemical shifts at -175 ppm in ¹⁹F NMR and 0.7 ppm in ¹¹B NMR.



Scheme 4. Bottom: Synthesis of fluoroborate **2**-F; Top: NMR evidence for the generation of [**1**-F]⁻. NMR spectra are reported in *d*₆-DMSO.

UV-vis spectroscopy was employed to monitor fluoride binding upon incremental additions of TBAF to a CH₂Cl₂ solution of [2]BF₄. As the reaction proceeded, the low-energy absorption band assigned to the acridinium chromophore in the 400-480 nm range progressively disappeared. At the same time, a new, red-shifted broad band centered at 495 nm emerged,

leading to a visible color change (Figure 2). As supported by calculations (vide infra), this low energy feature is a charge-transfer involving the fluoroborate moiety as a donor and the acridinium as the acceptor. Similar CT bands were obtained with pyridinium boranes III and IV upon fluoride binding.^{7, 13, 17} Fitting the absorbance data obtained at 505 nm in CH₂Cl₂ indicates that the fluoride binding constant exceeds 10⁷ M⁻¹ (Figure 2).^{5, 18} The elevated fluoride binding constant is comparable to that of other cationic boranes which also display an electrostatically enhanced affinity for the fluoride anion.^{8, 19, 20} ¹H NMR investigation indicates that the acridinium moiety remained untouched even in the presence of excess fluoride. This lack of a reaction serves as a reminder that acridinium cation is a very stable carbenium as indicated by the pK_{R+} of 11.0 determined for 9-phenyl-10-methylacridinium.²¹ Interestingly, fluoroborate **2**-F slowly converted into the borate carbinol [1-F] in DMSO as indicated by new peaks in the ¹H NMR spectrum after 12 hours (Scheme 4). This transformation was accompanied by the formation of a minor and unidentified impurity giving rise to weak resonances in the ¹H NMR spectrum. To verify this conclusion, the fluoride adduct [1-F] was independently generated by adding KF to a DMSO solution of carbinol 1. The resulting ¹H NMR spectrum is consistent with that observed upon decomposition of 2-F (Scheme 4).

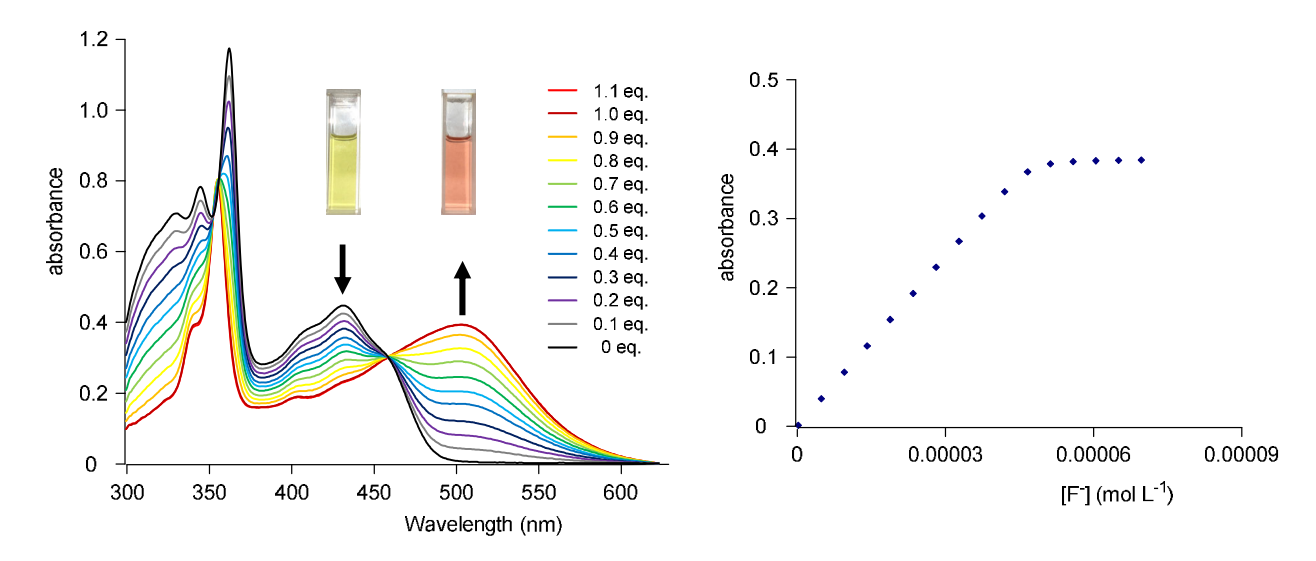


Figure 2. Conversion of [2]BF₄ (5.0×10^{-5} M) to 2-F monitored by UV-vis spectroscopy in CH₂Cl₂ upon incremental addition of a TBAF solution (5.0×10^{-3} M in CH₂Cl₂). The presence of two well-anchored isosbestic points at 457 and 352 nm is indicative of a clean 1:1 binding process.

To gain a better understanding of the chromophores, density functional theory (DFT) computations of $[2]^+$ and 2-F were performed. The structures of $[2]^+$ and 2-F were optimized (functional: mpw1pw91, 6-311G(d,p) for all atoms) using the Solvation Model Based on Density (SMD) model and dichloromethane as the solvent. Inspection of the frontier orbitals shows that the lowest unoccupied molecular orbital (LUMO) of each molecule is localized on the acridinium unit of the molecule while the orbitals from the highest occupied molecular orbital (HOMO) to HOMO-3 reside primarily on the mesityl rings (see SI for details). The electronic transitions in $[2]^+$ and 2-F were determined using time-dependent DFT (TD-DFT) methods which closely matched the experimentally obtained spectroscopic features. These calculations support the presence of an intramolecular charge-transfer from the dimesitylboryl/fluoroborate unit to the acridinium moiety, and they indicate that the main contribution to the spectroscopic feature in $[2]^+$ is a HOMO-1 \rightarrow LUMO transition and a HOMO-2 \rightarrow LUMO transition in the case of 2-F (Figure 3 and SI). The energy gap involved in the electronic transition noticeably

decreased on going from the cationic borane [2]⁺ (3.29 eV) to the corresponding fluoroborate species 2-F (3.01 eV). The narrowing of this energy gap, and hence the red shift observed in the UV-vis spectrum, is driven by a destabilization of the donor orbital which resides in the dimesitylfluoroborate moiety of 2-F.

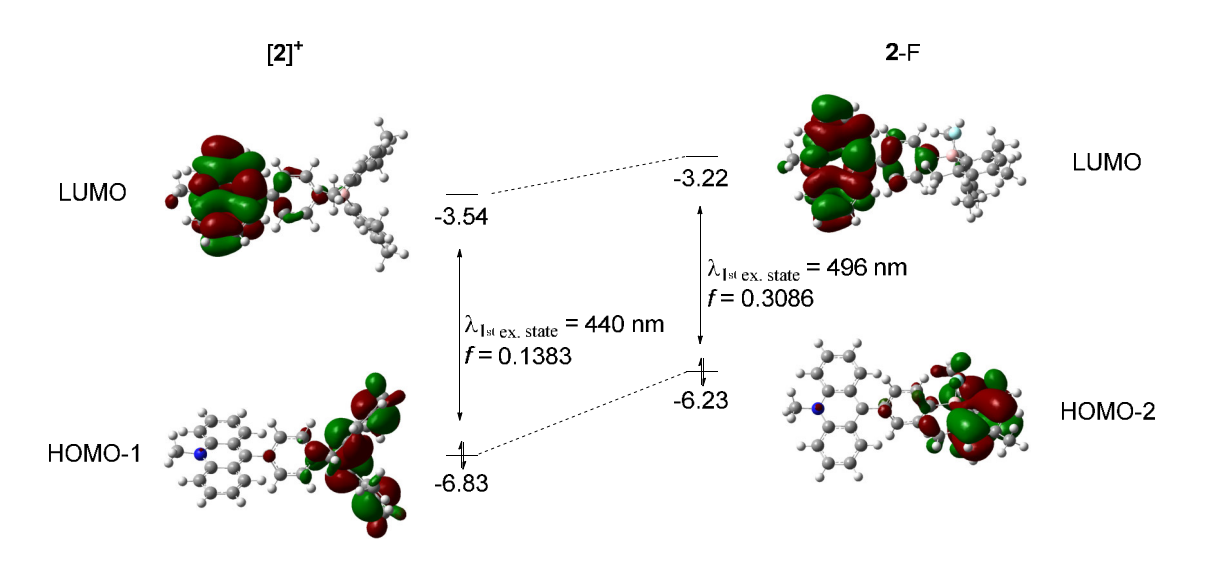


Figure 3. Interpretation of the molecular orbitals of [2]⁺ and 2-F participating in the electronic transition along with relative energy gap given in eV. Isosurface values are set at 0.02. The TD-DFT calculated excitation energies and corresponding oscillator strengths are also provided.

4. Electrochemical properties of [2]BF₄ and 2-F

Because this bifunctional complex possesses a redox-active acridinyl functionality, we decided to investigate the electrochemical properties of the system. We recorded a cyclic voltammogram (CV) of [2]BF₄ in CH₂Cl₂ where two distinct reduction waves were observed at $E_{1/2} = -0.99$ V and -1.77 V (vs. Fc/Fc⁺) (Figure 4 and SI). The first wave is assigned to the reversible reduction of the acridinium unit to produce the corresponding radical, 2° (Figure 5). The potential of this reduction is comparable to that reported for acridinium cations (-0.95 V)^{22, 23} in agreement with

the lack of significant conjugation between the acridinium cation and the boryl unit. Immediately after the *in situ* addition of TBAF to a dichloromethane solution of [2]BF₄, both reduction waves are cathodically shifted to $E_{1/2}$ values of -1.11 V and -2.05 V vs. Fc/Fc⁺, respectively. This electrochemical response in going from [2]BF₄ to 2-F supports the idea that fluoride binding elevates the LUMO energy, leading to a more electron rich acridinium center.

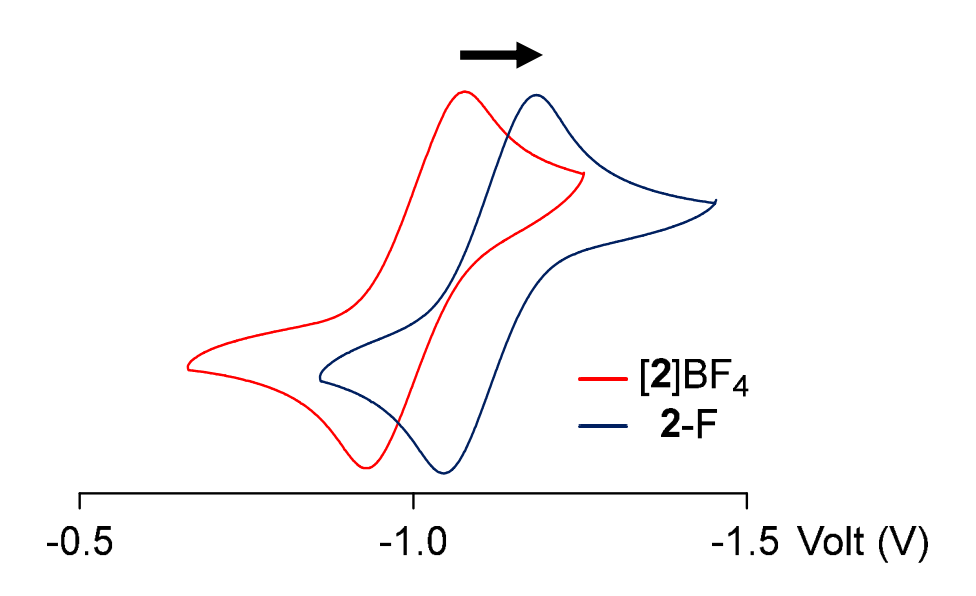


Figure 4. CV of [2]BF4 and 2-F in CH₂Cl₂ with a glassy carbon working electrode; scan rate 100 mV s⁻¹, 0.1 M NBu₄PF₆. All reduction potentials are reported with respect to the Fc/Fc⁺ redox couple

Because the reversibility of the first reduction wave suggested that radical 2' is stable, we attempted its chemical generation. Following previous procedures, 23, 24 [2]BF4 was reduced using magnesium pellets in acetonitrile to form the desired radical as indicated by the dramatic color change from yellow to deep purple. When analyzed by EPR spectroscopy, radical 2' exhibited a signal distinct to acridinyl-based radicals which was characterized by the hyperfine coupling constants shown in Figure 5. The computed spin density map of 2' suggests that the unpaired electron is located predominantly on the acridinyl ring with little contribution from the

dimesitylboryl group (Figure 5 and SI). This result again emphasizes the poor π conjugation between the acridinyl and dimesitylboryl moieties found XRD analysis of [2]BF₄.

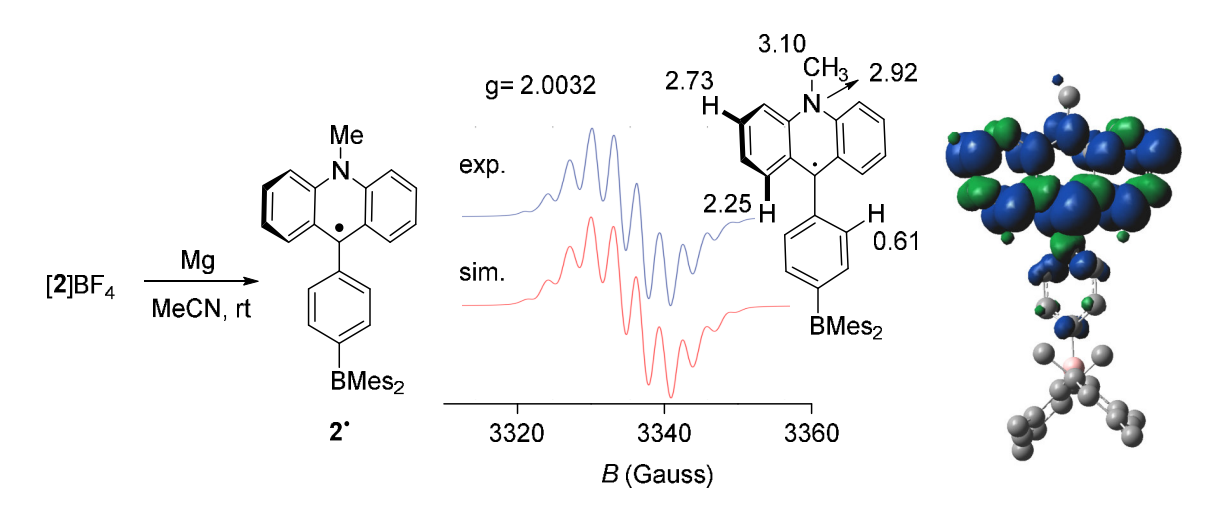


Figure 5. Left: synthesis of 2. Center: EPR spectrum of 2 and hyperfine coupling constants. Right: Spin density map of 2.

In summary, we reported an acridinium borane [2]BF₄ as a turn-on fluoride anion sensor with a binding constant exceeding 10⁷ in CH₂Cl₂. The conversion of [2]BF₄ to fluoroborate 2-F was monitored using UV-vis spectroscopy, revealing a red shift of the low-energy charge-transfer band upon fluoride binding. This result was further supported computationally with a noticeable decrease in the electronic transition gap after conversion of the borane into a fluoroborate moiety. Finally, the generation and characterization of radical 2^{*} demonstrated an acridinyl-based radical with a poor conjugation between the two functional groups.

5. Experimental

General Considerations. Air-sensitive compounds were handled under a N₂ atmosphere using standard Schlenk and glovebox techniques. 4-(Bromophenyl)-dimesitylborane²⁵ and N-methyl acridone²⁵ were prepared following published procedures. Tetrabutylammonium fluoride trihydrate (TBAF•3H₂O), potassium fluoride (KF) and magnesium pellet were obtained commercially and used without further purification. THF was dried by refluxing over Na/K under a N₂ atmosphere. Acetonitrile and dichloromethane were dried by refluxing over CaH₂ under a N₂ atmosphere.

NMR spectra were recorded at room temperature using a Varian Inova 500 FT NMR (499.23 MHz for ¹H and 469.81 MHz for ¹⁹F) spectrometer, a Bruker Avance 500 NMR spectrometer (500.13 MHz for ¹H and 126.76 MHz for ¹³C), or a Bruker Ascend 400 NMR spectrometer (400.20 MHz for ¹H and 128.36 MHz for ¹¹B). Chemical shifts are given in ppm. ¹H and ¹³C signals were referenced to residual ¹H or ¹³C solvent signals.²⁶ ¹¹B signals are referenced using BF₃·Et₂O solution as external standard (0.0 ppm). The ¹⁹F signals are referenced using C₆F₆ as a secondary external standard set at -161.64 ppm vs. CFCl₃.²⁷ Mass spectrometry analyses were performed in-house.

Crystallography. The crystallographic measurements were performed at 110 K using a Bruker D8 Quest (Mo source) diffractometer equipped with Photon III detectors. Semi-empirical absorption corrections were applied using the Bruker SADABS software package.²⁸ The structures were solved by direct methods with SHELXT²⁹ to locate all non-hydrogen atoms. Subsequent refinement using a difference map on F² with the SHEXL package³⁰ allowed for the location of the remaining non-hydrogen atoms which were refined anisotropically. H atoms

were added at calculated positions using a riding model. CCDC 2159106-2159107 contain the supplementary crystallographic data for this paper. These data can be obtained free of charge via www.ccdc.cam.ac.uk/data request/cif, or by emailing data request@ccdc.cam.ac.uk.

Electrochemical Measurements. All electrochemical experiments were performed with an electrochemical analyzer from CH Instruments (Model 615 A) with a standard 3-electrode system: An Ag/AgNO₃ reference electrode, a glassy carbon working electrode, and a platinum wire auxiliary electrode. The electrodes were immersed in a solution (10 mL) containing supporting electrolyte ⁿBu₄NPF₆ (0.1 M) and compound [2]BF₄ or 2-F (0.001 M in CH₂Cl₂). The electrolyte, ⁿBu₄NPF₆, was obtained commercially and was used without further purification. All solutions were degassed before measurement. In all cases, the spectrum was obtained using a scan rate = 0.1 V s⁻¹ and ferrocene as an internal standard, and all reduction potentials are reported with respect to the Fc/Fc⁺ redox couple.

Theoretical Calculations. All calculations were performed using DFT methods as implement in the Gaussian 09 software.³¹ The level of theory employed was as follows: Functional: MPW1PW91; Basis sets: 6-311g(d,p). Frequency calculations conducted using at the same level of theory found no imaginary frequencies. Time-dependent DFT (TDDFT) calculations were conducted at the same level of theory as for the optimization and with application of the SMD (solvent = dichloromethane). Molecular orbitals and spin density map were visualized using GaussView 5.0 program.

EPR spectroscopy. Solution EPR measurements were carried out on a Bruker EMX X-band spectrometer. Samples containing a 10⁻⁴ M concentration of **2** were prepared by *in situ* by reduction of [**2**]BF₄ (60.5 mg, 0.1 mmol) with Mg pellets (2.7 mg, 0.11 mmol) in MeCN over the course of two hours. An aliquot of this solution (0.05 mL) was diluted in THF (2 mL). A portion of the resulting solution was then transferred to a 2 mm EPR tube inside a glove box. The EPR spectra were obtained at room temperature with a microwave power of 1.987 mW, a modulation amplitude of 0.1 G, a time constant of 163.84 ms, and a sweep time of 60.0 s. The EPR spectrum was simulated using the EasySpin software package in MATLAB, yielding the hyperfine coupling constants listed in Figure 5.

Syntheses.

Synthesis of 1. nBuLi (2.5 M in hexane, 1.19 mL, 2.97 mmol) was added to a solution of (4-bromophenyl)dimesitylborane (1.00 g, 2.48 mmol) in THF (15 mL) at -78°C. The solution was stirred for 1 hour before being combined with a solution of N-methylacridone (0.62 g, 2.97 mmol) in THF (5 mL). After stirring for 1 hour at -78°C, the reaction was allowed to warm to room temperature. It was stirred for an additional 12h at this temperature before being quenched with NH₄Cl_(aq) (20 mL). Extraction with Et₂O (2 x 10 mL) produced an organic phase that we treated with MgSO₄ and brought to dryness under vacuum to afford a crude solid which was washed with acetonitrile (2 x 5 mL). This procedure afforded compound 1 as a white solid (0.97g, 1.81 mmol, 73%). Single crystals suitable for XRD analysis were obtained by slow diffusion of pentane into a CH₂Cl₂ solution of 1 at room temperature. ¹H NMR (CDCl₃, 500.13 MHz) δ 7.37-7.43 (m, 4 H, Ar-*H*), 7.28-7.35 (m, 4 H, Ar-*H*), 7.05 (d, J = 8.2 Hz, 2H, Ar-*H*), 6.95 (td, J = 7.3, 0.9 Hz, 2H, Ar-*H*), 6.78 (s, 4H, Ar-*H*), 3.52 (s, 3H, -NCH₃), 2.41 (s, 1H, Ar₃CO*H*), 2.28 (s,

6H, ArC*H*₃), 1.98 (s, 12H, ArC*H*₃). ¹¹B{¹H} NMR (CDCl₃, 128.36 MHz) δ 77.18. ¹³C{¹H} NMR (CDCl₃, 125.76 MHz) δ 150.86 (s), 144.37 (br, s), 141.97 (br, s), 140.89 (s), 140.16 (s), 138.61 (s), 136.15 (s), 128.79 (s), 128.62 (s), 128.24 (s), 127.95 (s), 126.29 (s), 120.62 (s), 112.47 (s), 73.76 (s), 33.56 (s), 23.58 (s), 21.33 (s). HRMS (ESI-): [M-H]⁻ C₃₈H₃₇NBO calc. 534.2963 m/z, found 534.2980 m/z.

Synthesis of [2]BF4. The title compound was prepared by adding HBF4*Et₂O (52% w/w in Et₂O, 58 mg, 0.36 mmol) to a solution of **1** (200 mg, 0.36 mmol) in Et₂O (10mL) at ambient temperature. The resulting mixture which turned rapidly from colourless to bright yellow was stirred for another hour before being brought to dryness. The yellow residue was washed with Et₂O (2 x 10 mL) to afford [**2**]BF4 as a yellow solid (214 mg, 0.35 mmol, 95% yield). Single crystals suitable for XRD analysis were obtained by slow diffusion of pentane to a CH₂Cl₂ solution of [**2**]BF4 at room temperature. ¹H NMR (CD₃CN, 499.29 MHz) δ 8.78 (d, J = 9.1 Hz, 2H, Ar-H), 8.40 (ddd, J = 9.5, 6.6, 1.3 Hz, 2H, Ar-H), 7.95 (dd, J = 8.9, 1.2 Hz, 2H, Ar-H), 7.77-7.85 (m, 4H, Ar-H), 7.47 (d, J = 8.0 Hz, 2H, Ar-H), 6.89 (s, 4H, Ar-H), 5.05 (s, 3H, -NCH₃), 2.34 (s, 6H, ArCH₃), 2.13 (s, 12H, ArCH₃). ¹¹B{¹H} NMR (CD₃CN, 128.36 MHz) δ 73.56 (br, s), -0.97 (s, BF4). ¹³C{¹H} NMR (CD₃CN, 125.76 MHz) δ 162.35 (s), 149.15 (br, s), 142.69 (s), 142.43 (br, s), 141.86 (s), 140.54 (s), 139.76 (s), 137.36 (s), 136.53 (s), 130.96 (s), 130.70 (s), 129.33 (s), 128.96 (s), 126.94 (s), 119.54 (s), 29.81 (s), 23.79 (s), 21.28 (s). HRMS (ESI+): [M-BF4]⁴ C₃₈H₃₇NB calc. 518.3014 m/z, found 518.2995 m/z.

Generation of [1-F]K. The title compound was prepared and characterized by multinuclear NMR spectroscopy in situ by addition of KF to a solution of 1 in d_6 - DMSO. ¹H NMR (d_6 -

DMSO, 500.13 MHz) δ 7.51 (dd, J = 7.7, 1.4 Hz, 2H, Ar-H), 7.21 (ddd, J = 8.9, 6.8, 1.5 Hz, 2H, Ar-H), 7.02 (d, J = 8.3 Hz, 2H, Ar-H), 6.91 (td, J = 7.6, 0.7 Hz, 2H, Ar-H), 6.86-7.40 (br, s, 1H, Ar-H), 6.68 (br, s, 3H, Ar-H), 6.32 (s, 4H, Ar-H), 5.75 (s, 1H, Ar₃COH), 3.39 (s, 3H, -NCH₃), 2.04 (s, 6H, ArCH₃), 1.75 (s, 12H, ArCH₃). 11 B $\{^{1}$ H $\}$ NMR (d₆- DMSO, 128.40 MHz) δ 0.52 (s, Ar₃BF). 13 C $\{^{1}$ H $\}$ NMR (d₆- DMSO, 125.76 MHz) δ 155.46 (br, s), 142.44 (s), 140.63 (s), 139.84 (s), 132.12 (s), 132.07 (s), 130.85 (s), 129.98 (s), 127.76 (s), 127.11 (s), 126.98 (s), 123.39 (s), 119.49 (s), 111.77 (s), 71.89 (s), 33.10 (s), 24.79 (s), 24.76 (s), 20.51 (s). 19 F $\{^{1}$ H $\}$ NMR (d₆- DMSO, 469.81 MHz) δ -174.90 (s, Ar₃BF). HRMS (ESI-): [M-K]⁻ C₃₈H₃₈BFNO calc. 554.3025 m/z, found 554.3039 m/z.

Synthesis of 2-F. The title compound was prepared by addition of TBAF trihydrate (31.5 mg, 0.1 mmol) into a CH₂Cl₂ solution of [**2**]BF₄ (60.5 mg, 0.1 mmol). During the reaction an orange solid gradually formed. Upon completion, the precipitated solid was collected, washed with Et₂O (5 mL) to afford **2-**F as an orange powder. (49.8mg ,93%). ¹H NMR (d_6 - DMSO, 500.13 MHz) δ 8.80 (d, J = 9.2 Hz, 2H, Ar-H), 8.41 (t, J = 7.7 Hz, 2H, Ar-H), 8.11 (d, J = 8.6 Hz, 2H, Ar-H), 7.94 (t, J = 7.6 Hz, 2H, Ar-H), 7.81-8.01 (br, s, 1H, Ar-H), 7.19 (br, s, 3H, Ar-H), 6.46 (s, 4H, Ar-H), 4.87 (s, 3H, -NCH₃), 2.11 (s, 6H, ArCH₃), 1.95 (s, 12H, ArCH₃). ¹¹B{¹H} NMR (d_6 - DMSO, 128.40 MHz) δ 0.46 (s, Ar₃BF), -1.31 (s, BF₄). ¹³C{¹H} NMR (d_6 - DMSO, 125.76 MHz) δ 163.30 (s), 154.33 (br, s), 141.20 (s), 140.71 (s), 138.08 (s), 133.29 (br, s), 130.55 (s), 129.99 (s), 128.04 (s), 127.72 (s), 127.39 (s), 127.18 (s), 125.54 (s), 119.03 (s), 116.13 (s), 38.67 (s), 24.88 (s), 24.85 (s), 20.54 (s). ¹⁹F{¹H} NMR (d_6 - DMSO, 469.81 MHz) δ -148.32 (s, B F_4), -175.70 (s, Ar₃BF).

6. Acknowledgements

This work was supported by the National Science Foundation (CHE-2108728), the Welch Foundation (A-1423), and Texas A&M University (Arthur E. Martell Chair of Chemistry). We thank Logan Maltz for his help with the writing.

7. References

- 1. Fluorine and fluorides. Environmental Health Criteria 36, IPCS International Programme on Chemical Safety, World Health Organization 1984.
- 2. Fluorides. Environmental Health Criteria 227, IPCS International Programme on Chemical Safety, World Health Organization 2002.
- 3. Carton, R. J., Review of the 2006 United States National Research Council report: fluoride in drinking water. *Fluoride* **2006**, *39* (3), 163-172.
- 4. Yamaguchi, S.; Akiyama, S.; Tamao, K., Colorimetric Fluoride Ion Sensing by Boron-Containing p-Electron Systems. *Journal of the American Chemical Society* **2001**, *123* (46), 11372-11375.
- 5. Solé, S.; Gabbaï, F. P., A bidentate borane as colorimetric fluoride ion sensor. *Chemical Communications* **2004**, (11), 1284-1285.
- 6. Wade, C. R.; Broomsgrove, A. E. J.; Aldridge, S.; Gabbaï, F. P., Fluoride Ion Complexation and Sensing Using Organoboron Compounds. *Chemical Reviews* **2010**, *110* (7), 3958-3984.
- 7. Wade, C. R.; Gabbaï, F. P., Colorimetric turn-on sensing of fluoride ions in H₂O/CHCl₃ mixtures by pyridinium boranes. *Dalton Transactions* **2009**, (42), 9169-9175.
- 8. Kim, Y.; Gabbaï, F. P., Cationic Boranes for the Complexation of Fluoride Ions in Water below the 4 ppm Maximum Contaminant Level. *Journal of the American Chemical Society* **2009**, *131* (9), 3363-3369.
- 9. Hudnall, T. W.; Kim, Y.-M.; Bebbington, M. W. P.; Bourissou, D.; Gabbaï, F. P., Fluoride ion chelation by a bidentate phosphonium/borane Lewis acid. *Journal of the American Chemical Society* **2008**, *130* (33), 10890-10891.
- 10. Lee, M. H.; Agou, T.; Kobayashi, J.; Kawashima, T.; Gabbaï, F. P., Fluoride ion complexation by a cationic borane in aqueous solution. *Chemical Communications* **2007**, (11), 1133-1135.
- 11. Cao, D.; Zhao, H.; Gabbaï, F. P., A sandwich complex of trimesitylborane Mes₃B: synthesis, characterization and anion binding properties of Mes₂B[(h⁶-Mes)FeCp]⁺. *New Journal of Chemistry* **2011**, *35* (10), 2299-2305.
- 12. Wade, C. R.; Gabbaï, F. P., Cyanide anion binding by a triarylborane at the outer rim of a cyclometalated ruthenium(II) cationic complex. *Inorganic Chemistry* **2010**, *49* (2), 714-720.

- 13. Liu, X. Y.; Bai, D. R.; Wang, S., Charge-transfer emission in nonplanar three-coordinate organoboron compounds for fluorescent sensing of fluoride. *Angew. Chem.* 2008, 120, 4122-4126; **2006**, 45 (33), 5475-5478.
- 14. Zhao, H.; Gabbaï, F. P., On the Synergy of Coulombic and Chelate Effects in Bidentate Diboranes: Synthesis and Anion Binding Properties of a Cationic 1,8-Diborylnaphthalene. *Organometallics* **2012**, *31* (6), 2327-2335.
- 15. Bai, D.-R.; Liu, X.-Y.; Wang, S., Charge-transfer emission involving three-coordinate organoboron: V-shape versus U-shape and impact of the spacer on dual emission and fluorescent sensing. *Chemistry--A European Journal* **2007**, *13* (20), 5713-5723.
- 16. Dorsey, C. L.; Gabbaï, F. P., Synthesis and redox properties of a para-borylated phenylxanthenium cation. *Main Group Chemistry* **2010**, *9* (1-2), 77-85.
- 17. Jonker, S. A.; Ariese, F.; Verhoeven, J. W., Cation complexation with functionalized 9-arylacridinium ions: Possible applications in the development of cation-selective optical probes. *Recueil des Travaux Chimiques des Pays-Bas* **1989**, *108* (3), 109-115.
- 18. Lin, T.-P.; Nelson, R. C.; Wu, T.; Miller, J. T.; Gabbaï, F. P., Lewis acid enhancement by juxtaposition with an onium ion: the case of a mercury stibonium complex. *Chemical Science* **2012**, *3*, 1128-1136.
- 19. Chiu, C.-W.; Gabbaï, F. P., Fluoride Ion Capture from Water with a Cationic Borane. *Journal of the American Chemical Society* **2006**, *128* (44), 14248-14249.
- 20. Hudnall, T. W.; Gabbaï, F. P., Ammonium Boranes for the Selective Complexation of Cyanide or Fluoride Ions in Water. *J. Am. Chem. Soc.* **2007**, *129* (39), 11978-11986.
- 21. Bunting, J. W.; Meathrel, W. G., Quaternary Nitrogen Heterocycles. II. Kinetics of Reversible Pseudobase Formation from N-Methyl Heterocyclic Cations. *Canadian Journal of Chemistry* **1973**, *51* (12), 1965-1972.
- 22. Hogan, D. T.; Sutherland, T. C., Modern Spin on the Electrochemical Persistence of Heteroatom-Bridged Triphenylmethyl-Type Radicals. *The Journal of Physical Chemistry Letters* **2018**, *9* (11), 2825-2829.
- 23. Liu, W.-C.; Kim, Y.; Gabbaï, F. P., Conformational Switching through the One-Electron Reduction of an Acridinium-based, γ -Cationic Phosphine Gold Complex. *Chemistry A European Journal* **2021**, *27* (22), 6701-6705.
- 24. Chiu, C.-W.; Gabbaï, F. P., A 9-borylated acridinyl radical. *Angew. Chem. 2008, 120, 4122-4126;* **2007,** *46* (10), 1723-1725.
- 25. Wilkins, L. C.; Kim, Y.; Litle, E. D.; Gabbaï, F. P., Stabilized Carbenium Ions as Latent, Z-type Ligands. *Angew. Chem. 2008*, *120*, *4122-4126*; **2019**, *58* (50), 18266-18270.
- 26. Fulmer, G. R.; Miller, A. J. M.; Sherden, N. H.; Gottlieb, H. E.; Nudelman, A.; Stoltz, B. M.; Bercaw, J. E.; Goldberg, K. I., NMR Chemical Shifts of Trace Impurities: Common Laboratory Solvents, Organics, and Gases in Deuterated Solvents Relevant to the Organometallic Chemist. *Organometallics* **2010**, *29* (9), 2176-2179.
- 27. Rosenau, C. P.; Jelier, B. J.; Gossert, A. D.; Togni, A., Exposing the Origins of Irreproducibility in Fluorine NMR Spectroscopy. *Angew Chem Int Ed Engl* **2018**, *57* (30), 9528-9533.
- 28. Sheldrick, G. M., SADABS, Version 2007/4, Bruker Analytical X-ray Systems, Inc., Madison, Wisconsin, USA. 2007.
- 29. Sheldrick, G. M., SHELXT integrated space-group and crystal-structure determination. *Acta Crystallographica Section A* **2015**, *71* (Pt 1), 3-8.

- 30. Sheldrick, G. M. SHELXTL, Version 6.1, Bruker Analytical X-ray Systems Inc.: Madison, Wisconsin, USA, 2000.
- 31. Frisch, M. J.; Trucks, G. W.; Schlegel, H. B.; Scuseria, G. E.; Robb, M. A.; Cheeseman, J. R.; Scalmani, G.; Barone, V.; Mennucci, B.; Petersson, G. A.; Nakatsuji, H.; Caricato, M.; Li, X.; Hratchian, H. P.; Izmaylov, A. F.; Bloino, J.; Zheng, G.; Sonnenberg, J. L.; Hada, M.; Ehara, M.; Toyota, K.; Fukuda, R.; Hasegawa, J.; Ishida, M.; Nakajima, T.; Honda, Y.; Kitao, O.; Nakai, H.; Vreven, T.; Montgomery, J., J. A.; Peralta, J. E.; Ogliaro, F.; Bearpark, M.; Heyd, J. J.; Brothers, E.; Kudin, K. N.; Staroverov, V. N.; Kobayashi, R.; Normand, J.; Raghavachari, K.; Rendell, A.; Burant, J. C.; Iyengar, S. S.; Tomasi, J.; Cossi, M.; Rega, N.; Millam, J. M.; Klene, M.; Knox, J. E.; Cross, J. B.; Bakken, V.; Adamo, C.; Jaramillo, J.; Gomperts, R.; Stratmann, R. E.; Yazyev, O.; Austin, A. J.; Cammi, R.; Pomelli, C.; Ochterski, J. W.; Martin, R. L.; Morokuma, K.; Zakrzewski, V. G.; Voth, G. A.; Salvador, P.; Dannenberg, J. J.; Dapprich, S.; Daniels, A. D.; Farkas, Ö.; Foresman, J. B.; Ortiz, J. V.; Cioslowski, J.; Fox, D. J., *Gaussian 09*, Revision B.01, Gaussian, Inc.: Wallingford, CT: 2009.